Physica C 485 (2013) 168–176

Contents lists available at SciVerse ScienceDirect

Physica C

journal homepage: www.elsevier.com/locate/physc

Specific heat of $Mg(B_{1-x}C_x)_2$, $x = 0.05$, 0.1

R.A. Fisher [a,b], J.E. Gordon [c], F. Hardy [a,b,1], W.E. Mickelson [a,d,2], N. Oeschler [a,b,3], N.E. Phillips [a,b,*], A. Zettl [a,d]

[a] Lawrence Berkeley National Laboratory, USA
[b] Department of Chemistry, University of California, Berkeley, CA 94720, USA
[c] Physics Department, Amherst College, Amherst, MA 01002, USA
[d] Department of Physics, University of California, Berkeley, CA 94720, USA

ARTICLE INFO

Article history:
Received 28 June 2012
Received in revised form 27 November 2012
Accepted 10 December 2012
Available online 20 December 2012

Keywords:
C-doped MgB_2
Superconductivity
Two gaps
Electron density of states

ABSTRACT

We report measurements of the specific heat of two samples of carbon-doped MgB_2, $Mg(B_{1-x}C_x)_2$, $x = 0.05$ and 0.1, in magnetic fields to $\mu_0 H = 9$ T and at temperatures from ~1 K to somewhat above the critical temperature for superconductivity for each sample. The carbon doping reduced the critical temperature from 39 K for MgB_2 to 31.4 K and 19.7 K for the $x = 0.05$ and 0.1 samples, respectively. The results give the electron–phonon coupling and the electron density of states, including the individual contributions of the π and σ bands. These quantities are compared with theoretical calculations. The results also give the energy gaps on the π and σ bands, which are compared with other experimental determinations, and also with theoretical calculations that include predictions of the "merging" of the two gaps as a consequence of the band filling and increased interband scattering associated with doping.

1. Introduction

The initial interest in the discovery of superconductivity in MgB_2 [1] was focused on the remarkably high critical temperature, $T_c \sim 39$ K, which seemed to be inconsistent with the BCS phonon-mediated electron pairing, Although calculations soon showed that the BCS mechanism did account for the high T_c, the superconductivity is still of special interest for another reason: MgB_2 is an example of multi-band, multi-gap superconductivity, *with substantially different energy gaps on different sheets of the Fermi surface*. The possibility of multi-band superconductivity had been recognized theoretically much earlier [2,3], and general relations for the thermodynamic properties, including relations between the gaps and details of the specific heat, had been derived [4]. However, MgB_2 was the first example in which the thermodynamic properties clearly show the presence of significantly different energy gaps on the different electron bands. The difference in the gaps makes possible the experimental separation of the contributions of the different bands to the thermodynamic properties. Specific-heat measurements [5,6] gave the first experimental evidence of two gaps, and their analysis with the α model [7], as extended to a two-band superconductor [8], gave values of the relevant parameters consistent with other experiments and theoretical calculations [9]. Measurements of the specific heat have a special role in such investigations for several reasons: they give information about the electron density of states (EDOS) that is not readily obtained from other measurements; whereas most other measurements that give information about the energy gaps are sensitive to surface properties, the specific heat is a bulk property. Doped samples of MgB_2 present a unique opportunity to study the effects of band filling, interband coupling, and interband scattering in a well understood two-band superconductor. As in the case of MgB_2 itself, specific-heat measurements can be expected to make a useful contribution to research on the doped materials.

In this paper measurements of the specific heat of two carbon-doped MgB_2 samples are reported, and parameters that characterize the electron contributions are compared with other experimental results and theoretical predictions. (Different values of those parameters, derived in a preliminary analysis of the data, were given in a conference report [10]. The preliminary analysis was based on the assumption that the zero-field, "residual" density of states was associated with non-superconducting regions of the $Mg(B_{1-x}C_x)_2$. Subsequent X-ray measurements showed that the impurity phase was MgB_2C_2, which would have a different lattice specific heat. The differences between the parameters reported here and those in the conference report are a consequence of corrections for the contribution of MgB_2C_2 to the measured specific heat, and a more rigorous separation of the lattice and electron contributions, which is described in Section 4.2. Miscommunication

* Corresponding author at: Department of Chemistry, University of California, Berkeley, CA 94720, USA. Tel.: +1 510 642 4855.
E-mail address: nephill@berkeley.edu (N.E. Phillips).
[1] Current address: Forschungszentrum Karlsruhe, Institut fur Festkorperphysik, 76021 Karlsruhe, Germany.
[2] Current address: Center of Integrated Nanomechanical Systems, University of California, Berkeley, CA 94720, USA.
[3] Current address: Infineon Technologies, Max-Planck-Str. 5, 59581 Warstein, Germany.

0921-4534/$ - see front matter © 2012 Elsevier B.V. All rights reserved.
http://dx.doi.org/10.1016/j.physc.2012.12.004

over notation led to an error, by a factor two, in the carbon content of the samples in the conference report.) Following an outline of some of the theoretical considerations in the remainder of this section, brief descriptions of the samples and the measurements are given in Sections 2 and 3. The relations used in the analysis of the data are summarized in Section 4.1. The presence of a nonsuperconducting impurity, MgB_2C_2, required a three-step process to obtain the contributions of the two bands to the electron specific heat: the lattice and electron contributions to the specific heat of the samples as measured were separated, and the electron specific heat corrected for the contribution of the MgB_2C_2, as described in Section 4.2; the superconducting-state electron specific heat of the $Mg(B_{1-x}C_x)_2$ was then analyzed to separate the contributions of the two bands, as described in Section 4.3. The results of the measurements and their analysis are compared with theoretical calculations and other experimental results in Sections 5.1 and 5.2, and summarized in Section 6.

MgB_2 comprises graphite-like hexagonal layers of B atoms separated by layers of Mg ions that are lined up with the centers of the boron hexagons. Because only s and p electrons are involved, band-structure calculations are straightforward and the results are relatively reliable. There is general agreement among the theoretical results, and also good agreement between theory and experiment. The Fermi surface consists of two tubular networks, the π bands, derived from the three-dimensional boron p_z orbitals, and two concentric cylindrical elements, the σ bands, derived from the quasi two-dimensional boron $p_{x,y}$ orbitals [11–15]. Both σ bands are hole like; one of the π bands is hole like and the other electron like. Although there are four distinct sheets of the Fermi surface, the superconducting-state energy gaps on each pair of bands are similar [15], and for the purpose of comparing theoretical predictions with thermodynamic properties MgB_2 can be regarded as a two-band superconductor. The E_{2g} phonon mode, which involves stretching of the bonds in the boron planes, couples strongly with the σ bands. It produces the larger of the two gaps, on the σ bands, and plays a major role [11,12,14,16] in producing the high T_c. The phonons couple weakly with the π bands, and relatively weak interband coupling also contributes to the smaller π-band gap. First principles calculations of the specific heat [15,17] show evidence of the major two-gap features observed experimentally [9].

The only widely studied dopants are Al on the Mg sites, and C on the B sites. In both cases electrons are added to the Fermi sea, and T_c decreases with increasing concentration of dopant. The band filling associated with doping, particularly in the σ band, can be expected to be important in determining the nature of the superconductivity. One suggestion [18] is that the decrease in T_c with doping is mainly a band-filling effect. For a multiband superconductor nonmagnetic scattering centers can be pair breaking and can also have an effect on the nature of the superconducting condensate on different sheets of the Fermi surface [19]. Interband scattering in a two-gap superconductor is also expected to reduce T_c, and to equalize the two gaps [20,21]. Mazin et al. [22] suggested that in the absence of observed correlations of T_c with resistivity in MgB_2 samples the case for two-gap superconductivity was not settled, but explained this apparent paradox on the basis of weak interband scattering. In any case, interband scattering can be expected to be stronger in the doped samples.

2. Samples

The samples were made by heating Mg turnings and B_4C powder, an approach that was first used by Mickelson et al. [23]. X-ray diffraction studies show that the C-doped samples produced by this method consist of two phases, a distorted MgB_2 structure and MgB_2C_2, which is nonsuperconducting [23,24]. The presence of substantial amounts of MgB_2C_2 seems to be a common feature of samples produced by this method [23–25]. Neutron diffraction measurements showed the presence of 7% MgB_2C_2 in another $x = 0.1$ sample [26]. For the samples studied in this work, powder X-ray diffraction measurements gave estimates of ∼6% and ∼10% for the MgB_2C_2 in the $x = 0.05$ and 0.1 samples, respectively. The presence of MgB_2C_2 in the samples also manifests itself as a normal-state-like contribution to the zero-field specific heat. The specific-heat measurements show the presence of paramagnetic impurities at the level of several tenths mol%. Straight-line, entropy-conserving constructions on the specific-heat anomalies at the transitions gave $T_c = 31.4$ K and 19.7 K for the $x = 0.05$ and 0.1 samples, respectively. For a sample with $T_c \sim 31$ K, essentially the same as that of the $x = 0.05$ sample, the lattice parameter is contracted from the 3.087 A for MgB_2 to 3.055 A, with no change in the b and c parameters [23]. Other properties of similar samples prepared by this method are reported elsewhere [23,24].

3. Specific-heat measurements

The specific-heat measurements were made in the same apparatus as those reported earlier for MgB_2 [6,9]. They were based on a heat-pulse technique with a mechanical heat switch to make and break thermal contact between the sample and a temperature-controlled heat shield. The measurements extend from ∼1 K to somewhat above T_c for each sample. They include measurements of the specific heat in magnetic fields, $C(H)$, in fields to $\mu_0 H = 9$ T. The results are shown as $[C(H) - C(9)]/T$ vs T. in Fig. 1. This figure gives an overview of the resolution of the H dependence of the "raw" data that would not be apparent in a plot of $C(H)/T$. Fig. 1b also permits a comparison with the specific heat of the only other sample on which such measurements have been reported, a sample with a similar T_c, for which the results were presented only in that form [25]. Comparisons of the data in different fields suggest that the 9-T data are low relative to the data in other fields by an amount that is estimated to be of the order of 1%. In the vicinity of T_c the discrepancy between the data in 9 T and the data in other fields can be seen in Fig. 1, where $[C(H) - C(9)]/T$ is consistently non-zero, and also in Fig. 2, where the 9-T data are consistently low. The H dependence of the entropy at a temperature slightly above T_c provides a measure of the consistency of the measurements in different fields: For the $x = 0.05$ sample at 35.0 K, for all H other than 9 T the entropies are within +0.3/−0.4% of their average; for 9 T the entropy is −1.1% relative to that average. For the $x = 0.1$ sample at 21.5 K, the comparable numbers are ±0.4% and −0.7%. Because of the discrepancy between the 9-T data and the data in other fields, the 9-T data have been omitted from all quantitative analyses, but they are included in the figures for the information they give on the 9-T transitions to the vortex state.

4. Analysis of specific-heat data

4.1. Relations used in fitting and interpreting the data

The analysis of the data is based on the usual assumption that $C(H)$ is the sum of an H-dependent electron component, $C_e(H)$, and an H-independent lattice component, C_{lat}. In addition, $C_e(H)$, which is designated C_{es} in the superconducting state and $C_{ev}(H)$ in the vortex state, is taken to be $C_{en} = \gamma T$ in the normal state. With the commonly used polynomial expression for C_{lat},

$$C_{lat} = B_3 T^3 + B_5 T^5 + B_7 T^7 + \cdots, \tag{1}$$

$$C(H) = C_e(H) + B_3 T^3 + B_5 T^5 + B_7 T^7 + \cdots,$$

and, in the normal state,

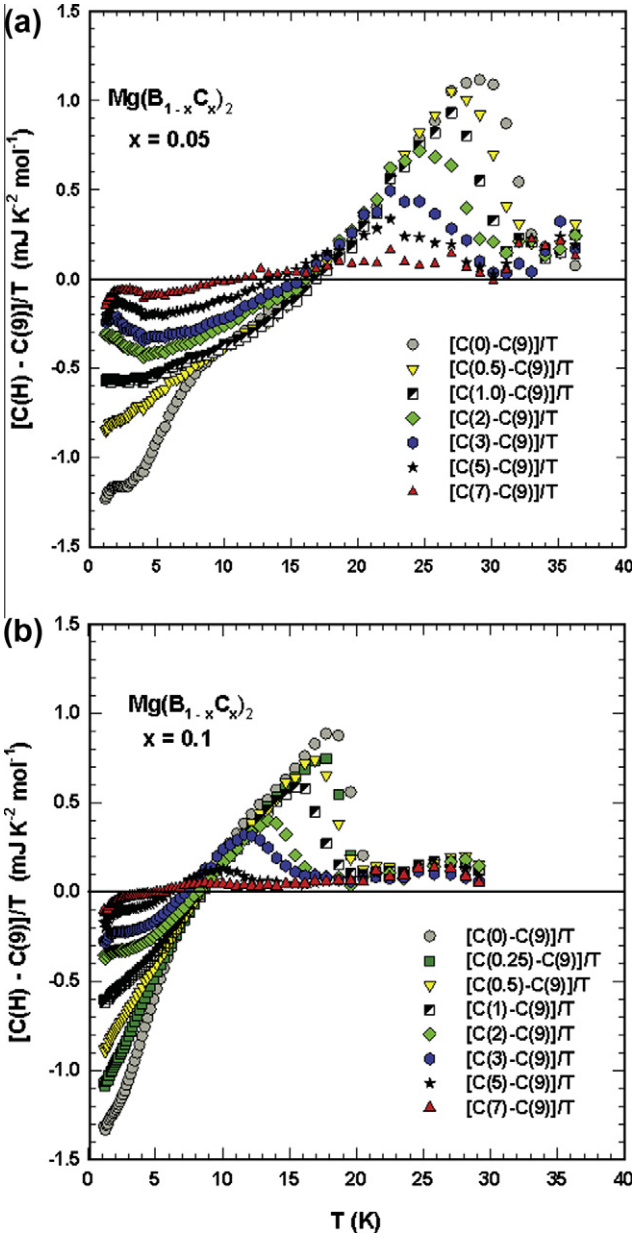

Fig. 1. The H dependence of the specific heat, as $[C(H) - C(9)]/T$, before subtraction of the paramagnetic-impurity contributions or any other analysis (see text for discussion): (a) for $x = 0.05$; (b) for $x = 0.1$. Fig. 1a permits a direct comparison with the specific-heat data in Ref. [25].

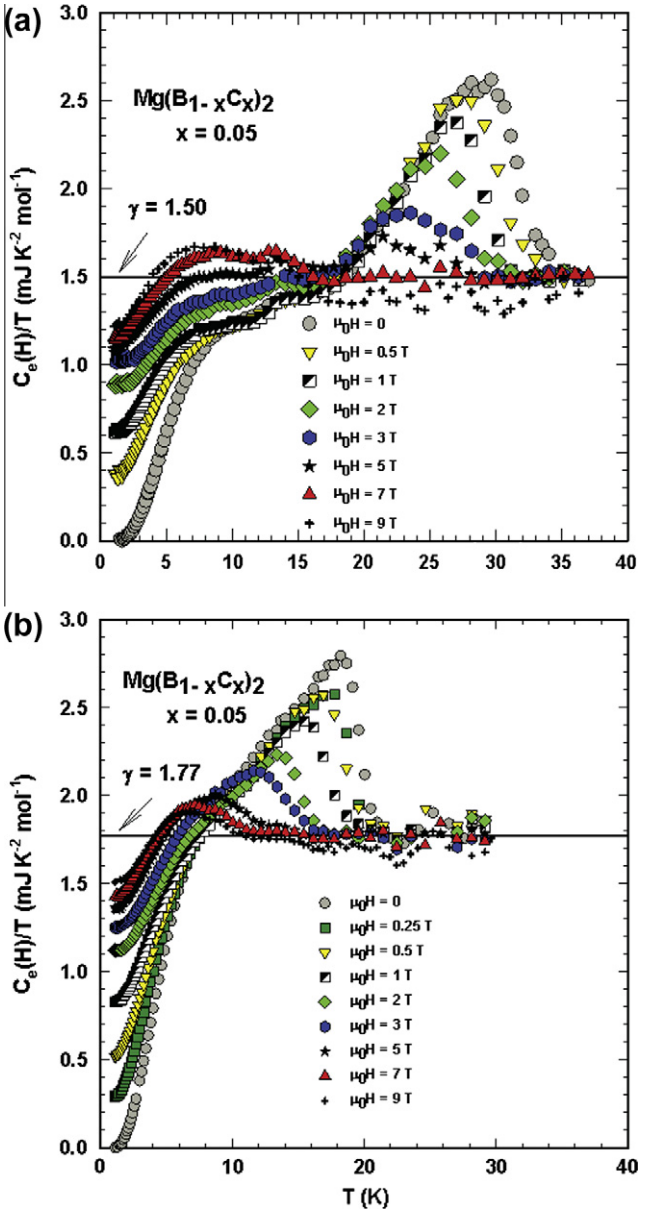

Fig. 2. The electron contributions to the specific heat: (a) for $x = 0.05$, (b) for $x = 0.1$.

$$C(H) = \gamma T + B_3T^3 + B_5T^5 + B_7T^7 + \cdots. \quad (2)$$

In these equations C_{lat} has the form expected for small amplitude vibrations in a monatomic harmonic lattice, i.e., for the acoustic modes in the low-temperature limit: The T^3 term represents the contribution of phonons in the low-frequency dispersionless limit, and the higher-order terms allow for the effects of dispersion. However, Eq. (2) is often used in an interval of temperature at higher temperatures, where optical modes make a contribution. In that case it is a convenient, but arbitrary, fitting expression; the parameters determined by the fit do not have the same physical meaning, and should not be expected to give correctly either C_{lat} at temperatures below the interval of the fit, or the lattice entropy in the interval of the fit.

In the vortex state

$$C_{eV}(H) = \gamma_v(H)T + a(H)\exp[-b(H)/T],$$

where the first term is the theoretically expected contribution of the vortex cores [27], and the second is an empirically determined approximation to the contribution of the superconducting condensate of a type II superconductor [28]. With the addition of C_{lat},

$$C(H) = \gamma_v(H)T + a(H)\exp[-b(H)/T] + B_3T^3 + B_5T^5 + B_7T^7 + \quad (3)$$

In the superconducting state

$$C(0) = C_{es} + B_3T^3 + B_5T^5 + B_7T^7 + \cdots, \quad (4)$$

where C_{es} is a function that goes exponentially to zero at low T. In the samples studied here, however, the MgB_2C_2 impurity phase contributes a "residual" EDOS and a normal-state-like contribution, $\gamma_r T$, which must be included in Eq. (4), to give

$$C(0) = \gamma_r T + C_{es} + B_3T^3 + B_5T^5 + B_7T^7 +, \quad (5)$$

where the first two terms represent the electron contributions of the two phases and the remaining terms represent C_{lat} *for the two-phase mixture*. As described below, the separation of the three contributions to $C(0)$ is based on the compositions of the samples as estimated from the the X-ray measurements and the values of γ_r.

The first step in analysis of the data was to make a correction for small H-dependent "upturns" in $C(H)/T$ below ~3 K, which appear as structure in $[C(H) - C(9)]/T$ in Fig. 1, and are associated with the magnetic impurities. For each H the data below ~4 K were fitted with the sum of the high-temperature tail of a Schottky anomaly and the first three terms of Eq. (3). The Schottky contributions were then subtracted and subsequent analysis was based on the data corrected in this way. (The second term in Eq. (3) was proposed as an empirical representation of that contribution to the specific heat for a single-gap superconductor. It cannot be expected to be a good approximation for a two-gap superconductor over the whole range of temperature to T_c, but it should be an adequate approximation in this low-temperature interval where only the small-gap band contributes.)

4.2. Electron contribution to the specific heat of $Mg(B_{1-x}C_x)_2$

The measured $C(H)$ has to be corrected for the contribution of the MgB_2C_2 to obtain $C(H)$ for $Mg(B_{1-x}C_x)_2$. Because data are available to make the correction for the electron component but not for the lattice component, the measured $C(H)$ was first analyzed to separate the electron and lattice components, and the electron component was then corrected for the MgB_2C_2 contribution. The high values of the critical fields, $H_{c2}(T)$, limit the temperature interval in which normal-state data are available for analysis with Eq. (2). In such a case constraining the fit to give the correct entropy at $T \sim T_c$ may give more reliable values of the parameters. That approach is used frequently, and was used successfully for MgB_2 [6]. It was also used in the preliminary analysis [10] of the data for the $Mg(B_{1-x}C_x)_2$ samples, but subsequent analyses showed that the derived values of the parameters were sensitive to the temperature interval of the fit and the number of terms in Eq. (2). Furthermore, the C_{lat} derived in this way, which gives entropy conservation at the zero-field transition as required, does not give entropy conservation at the in-field transitions at lower temperatures, i.e., it does not extrapolate to the correct C_{lat} at lower temperatures. Consequently, a different, two-step approach was used: First, a reasonably accurate value of B_3 was obtained by a fit with the first three terms in Eq. (3) to the 7-T data below ~4 K, where the second term in Eq. (3) is small and the fourth and higher-order terms are negligible. Eq. (2) with five terms in C_{lat}, but with B_3 fixed at the value obtained in the low-temperature fit to the 7-T data, was then used to make entropy-conserving fits to the 7-T, normal-state data. These fits were made in the intervals 15–37 K and 12–29 K for the $x = 0.05$ and 0.1 samples, respectively. They gave values of γ of 1.46 and 1.64 mJ K^{-2} mol^{-1} for the $x = 0.05$ and 0.1 samples, respectively. The values of B_3 obtained in the low-temperature fits and used in these fits were 0.0125 and 0.0175 mJ K^{-4} mol^{-1} for the $x = 0.05$ and 0.1 samples, respectively. For all fields other than 7 T the values of $\gamma_v(H)$ were obtained by fitting the data below ~4 K with the first three terms in Eq. (3), but with B_3 fixed at the values obtained in the low-temperature fits of the 7-T data. The $H = 0$ fits gave the values of γ_r, 0.074 and 0.171 mJ K^{-2} mol^{-1} for the $x = 0.05$ and 0.1 samples, respectively.

The concentrations of the impurity determined by the X-ray analysis and the residual EDOS, as measured by the values of γ_r, provide the basis for the correction of $C_e(H)$ for the contribution of the MgB_2C_2. If the X-ray concentrations were accurate they would be in approximately the same ratio as the values of γ_r. However, there is a discrepancy: estimates of γ for MgB_2C_2 based on the X-ray concentrations and the values of γ_r for the two samples differ by 34%. This implies errors of the order of 15% in the concentrations. Such errors in the X-ray results would not be surprising, and the values of γ_r can be expected to be more accurate measures of the *relative* concentrations of MgB_2C_2. Accordingly, the concentrations of MgB_2C_2 in the $x = 0.05$ and $x = 0.1$ samples were taken to be 5.0% and 11.6%, which keeps them similar in magnitude to the X-ray values, and eliminates the discrepancy in the apparent values of γ for MgB_2C_2. These concentrations and the values of γ_r were used to calculate the numbers of mols of each of the two components in the samples, and to correct the $C_e(H)$ measured for the sample to that for $Mg(B_{1-x}C_x)_2$. The uncertainty in the corrections is essentially that in the X-ray determinations of the magnitude of the MgB_2C_2 concentrations. With these corrections the values of γ for $Mg(B_{1-x}C_x)_2$ are 1.50 and 1.77 mJ K^{-2} mol^{-1} for $x = 0.05$ and 0.1, respectively. For each sample the measured value of B_3 is an average of those for MgB_2C_2 and $Mg(B_{1-x}C_x)_2$ weighted by their relative amounts in the sample. In the absence of the value of B_3 for MgB_2C_2 it is not possible to correct the measured value to obtain B_3 for the $Mg(B_{1-x}C_x)_2$.

$C_e(H)/T$ for $Mg(B_{1-x}C_x)_2$, obtained by subtraction of C_{lat} and correction for the contribution of the MgB_2C_2, is shown in Fig. 2. The specific-heat anomalies associated with the transitions to the vortex state, including those that occur at temperatures well below T_c, have plausible shapes and satisfy the entropy conservation requirement. The conservation of entropy in these transitions constitutes a test of the derived C_{lat} at temperatures well below T_c, and attests its general validity.

4.3. Two-gap analysis of the electron specific heat in the superconducting-state

For both samples C_{es}, shown in Fig. 2, deviates substantially from that given by BCS theory. The deviations are qualitatively similar to those for MgB_2, which are known to be a consequence of the presence of two different energy gaps. In such a case, one of the two gaps must be smaller than given by BCS theory, and the other larger [4]. At low temperatures the small-gap band dominates C_{es}; at T_c it makes a contribution to the discontinuity in $C_e(0)$ but the shape of the anomaly is determined mainly by the large gap. The standard way of interpreting the specific heat is by comparison with the α model [7]. Originally developed for single-band superconductors, the α model is based on the assumption that the temperature dependence of the gap is given by the BCS theory in the weak coupling limit, but the 0-K amplitude, $\Delta(0)$, is scaled by a factor that represents the strength of the coupling, $\alpha \equiv \Delta(0)/k_BT_c$, which has the value $\alpha_{BCS} = 1.764$ in the BCS theory. It was recognized in the earliest considerations of multiband superconductivity that interband coupling had to be taken into account, at least to ensure the equality of T_c in the different bands. In the application of the α model to a two-band superconductor it is assumed that each band makes an *independent* contribution to C_{es} scaled by the fraction of the total electron DOS derived from that band [8]. T_c is *assumed* to be the same in both bands but interband coupling is not otherwise taken into account. Nevertheless, the α model has been generally successful in representing specific-heat data and giving values of the parameters in reasonable agreement with other measurements and with theoretical calculations. Furthermore, its use in analyzing specific-heat data in multiband superconductors has been justified by comparison with the results obtained by solution of the Eliashberg equations [29]. Two-gap, α-model fits to C_{es} for both samples are shown in Fig. 3. They were obtained by adjusting the values of α and the fraction of the total EDOS for each band to obtain the best approximation to C_{es}. Theoretical calculations put the smaller gap on the π band and the larger gap on the σ band, which permits the association of each of the experimentally derived param-

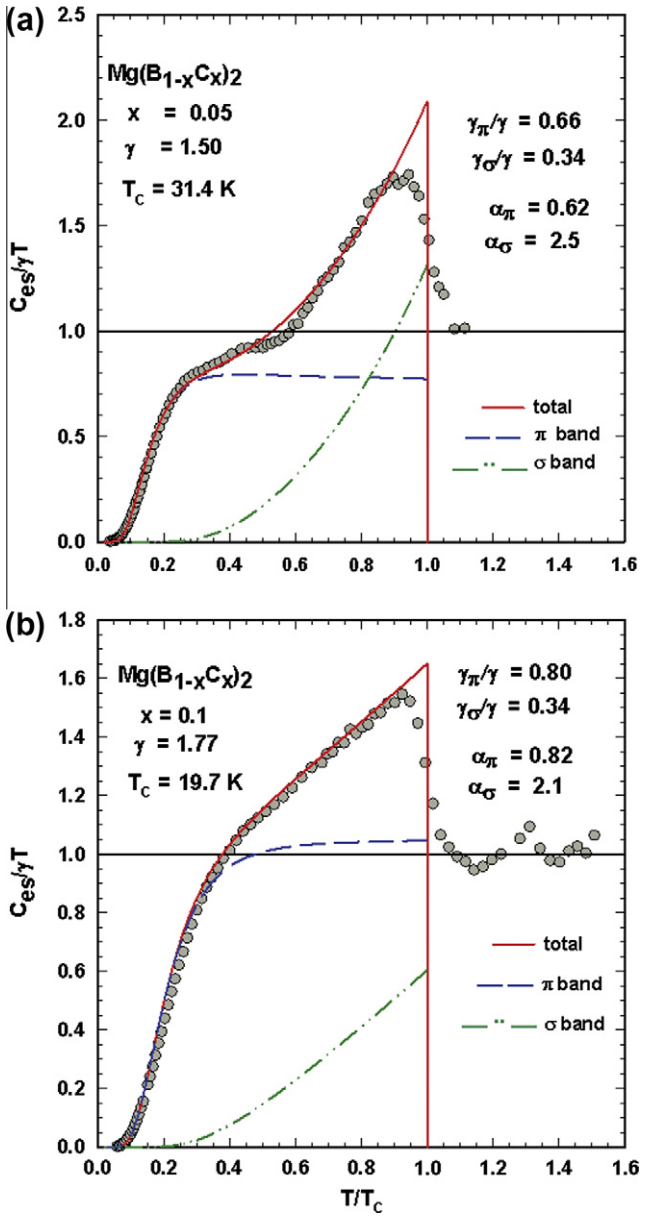

Fig. 3. Analysis of the superconducting-state electron specific heat into contributions associated with the σ and π bands: (a) for $x = 0.05$; (b) for $x = 0.1$. The curved lines represent the results of the fits: solid, for the total electron specific heat; dashed, for the π-band contribution; dash-dot, for the σ-band contribution.

Table 1
Parameters characteristic of the contributions of the π and σ bands to the electron specific heat: the coefficient of the total electron specific heat, in mJ K^{-2} mol^{-1}; the fractional contributions of the π and σ bands; the energy gaps, as represented by the values of α. The data for $x = 0$ are from Ref. [9].

x	γ	γ_π/γ	γ_σ/γ	α_π	α_σ
0	2.53	0.46	0.54	0.60	2.20
0.05	1.50	0.66	0.34	0.62	2.50
0.10	1.77	0.80	0.20	0.82	2.10

eters with the appropriate band. The parameters characterizing the gaps, α_π and α_σ, and the fractional EDOS, γ_π/γ and γ_σ/γ, are included in Table 1, where they are compared with those for MgB_2.

5. Discussion

5.1. Electron–phonon coupling, electron density of states, critical temperature, and energy gaps: comparisons with theoretical calculations and with other experimental results

Comparison of an experimental value of γ with theoretical calculations requires calculated values of both the band-structure EDOS, $N(E_F)$, and the electron–phonon coupling constant, λ, each of which contributes to γ. $N(E_F)$ is the "bare" EDOS, and gives the corresponding coefficient of the electron specific heat, $\gamma_0 = 2.357\, N(E_F)$, where γ_0 is in mJ K^{-2} mol^{-1} and $N(E_F)$ is in states eV^{-1} $cell^{-1}$. The experimental γ, which includes the phonon enhancement, is related to γ_0 by

$$\gamma = (1 + \lambda)\gamma_0 \tag{6}$$

Here and in the following, for convenience, each of the symbols $N(E_F)$, γ_0, λ, and γ is used to represent *either* the total of the quantity for the two bands *or* one of its single-band components. A relation of the form of Eq. (6) is valid in both cases. When needed for clarification or to specify a specific numerical quantity, subscripts π or σ are added for a single-band component, e.g., γ_π and γ_σ for the components of γ; $N_\pi(E_F)$ and $N_\sigma(E_F)$ for the components of $N(E_F)$.

Carbon doping of MgB_2 is expected to change parameters related to the superconductivity by band filling, with its attendant changes in the electron–phonon coupling, and also by increasing the interband scattering. Both effects are expected to reduce T_c. The interband scattering is expected to produce a merging of the two gaps, with the larger gap decreasing as the smaller gap increases. The band filling is expected to reduce both gaps. The relevant experimental results derived from the specific-heat data are summarized in Table 2 by the values of the π- and σ-band energy gaps at $T = 0$, Δ_π and Δ_σ, γ and its components, γ_π and γ_σ, and T_c. The evolution of γ_π, γ_σ, and γ with carbon doping is compared with theoretical calculations in Fig. 4 (there are no other experimental measurements). The x dependences of T_c and Δ_π and Δ_σ are compared with other measurements in Figs. 5 and 6.

Two groups have calculated the band structure, electron–phonon coupling, energy gaps, and T_c for $Mg(B_{1-x}C_x)_2$, but with somewhat different approaches: De la Pena-Seaman et al. [32,33] used the virtual-crystal approximation for the band-structure calculation; they solved the Eliashberg equations, taking the anisotropy of the Fermi surface into account, but without including interband scattering; they approximated the Coulomb pseudopotential with a value that had been derived for MgB_2. Ummarino et al. [34]. used the supercell approximation and included both interband scattering and an x-dependent Coulomb pseudopotential in several different ways. For undoped MgB_2, for which most of the differences in the two calculations should be irrelevant, the two groups report, respectively, $N(E_F) = 0.696$ and 0.70 states eV^{-1} $cell^{-1}$ Similar values have been reported by others, e.g., in the same units, 0.71 [11,35]; 0.710 [13,17]; 0.72 [22]. The well established band structure calculations used to obtain $N(E_F)$ for MgB_2, together with the consistency of the results, gives confidence in their accuracy. On the other hand, the spread in the calculated values of λ is considerably great-

Table 2
Parameters characteristic of the superconductivity in $Mg(B_{1-x}C_x)_2$: the energy gaps in the π and σ bands, in meV; the coefficient of the electron specific heat and the contributions of the π and σ bands, in mJ K^{-2} mol^{-1}; T_c, in K. The data for $x = 0$ are from Ref. [9].

x	Δ_π	Δ_σ	γ	γ_π	γ_σ	T_c
0	2.01	7.38	2.53	1.16	1.37	38.9
0.05	1.68	6.77	1.50	0.99	0.51	31.4
0.1	1.39	3.57	1.77	1.42	0.35	19.7

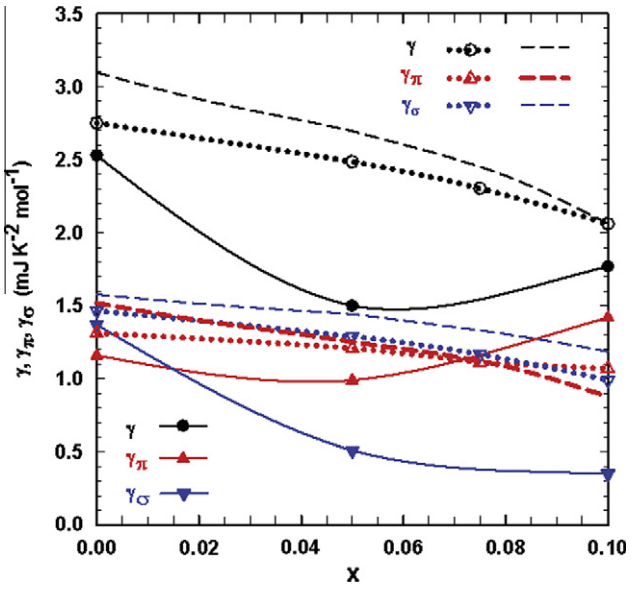

Fig. 4. The evolution of γ_π, γ_σ, and γ with C doping. The solid curves are guides to the eye. They connect solid symbols that represent the experimental results reported here for $x = 0.05$ and 0.1, and in Ref. [9] for $x = 0$. The dotted curves, which are also guides to the eye, connect open symbols that represent theoretical results calculated from the values of λ and $N(E_F)$ in Ref. [33]. The dashed curves represent the theoretical results shown in Figs. 1 and 2 of Ref. [34].

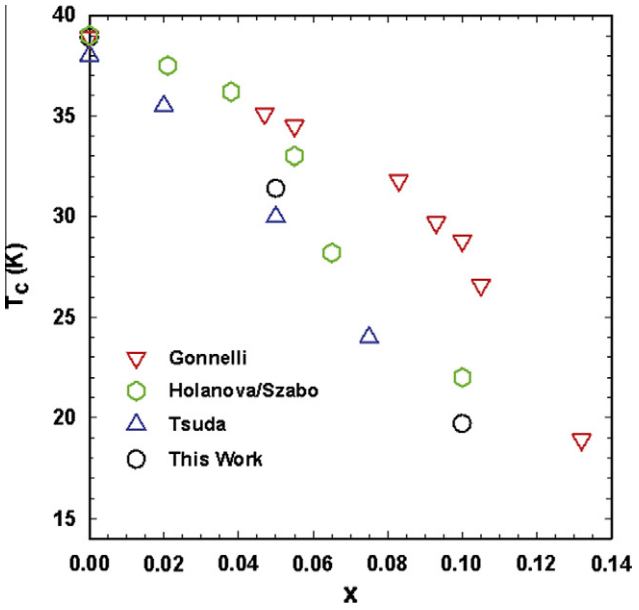

Fig. 5. Measurements of T_c as a function of carbon doping. The Gonnelli data are from Ref. [37], the Holanova/Szabo data from Refs. [38,39], and the Tsuda data from Ref. [40]. The point for this work at $x = 0$ is from Ref. [9].

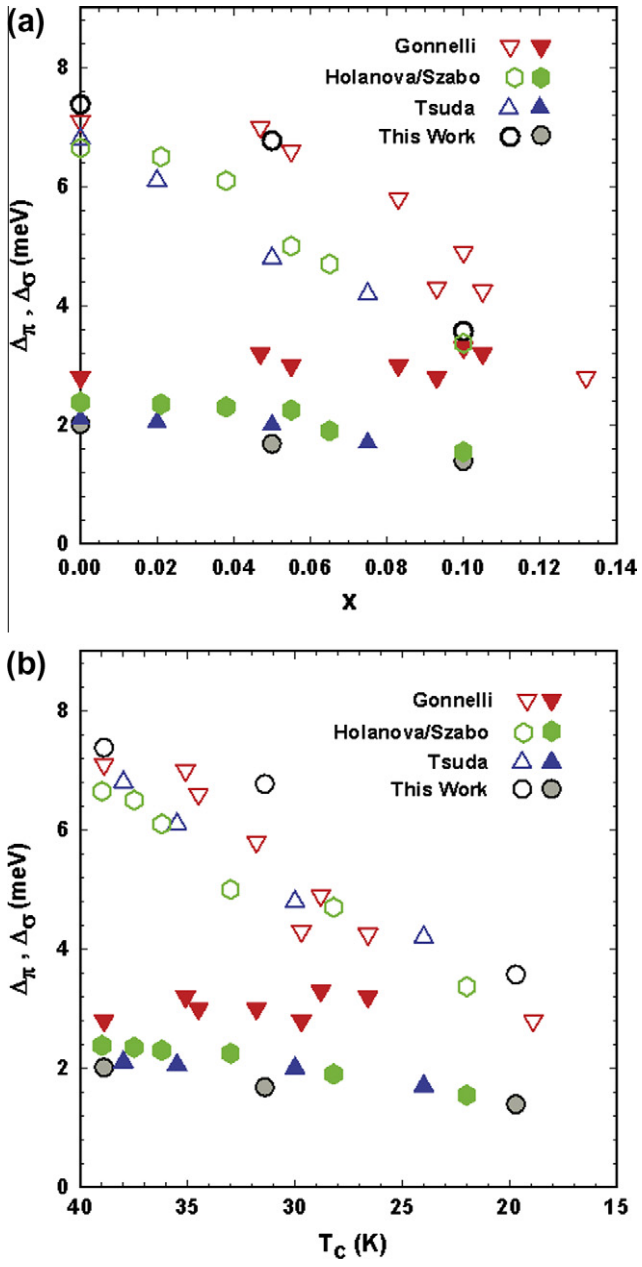

Fig. 6. Measurements of the energy gaps in the π and σ bands as a function of carbon doping: (a) plotted vs x, (b) plotted vs T_c. The Gonnelli data are from Ref. [37], the Holanova/Szabo data from Refs. [38,39], and the Tsuda data from Ref. [40]. With the exception of the Gonnelli point at $T_c = 18.9$ K and $x = 0.132$, for which only one gap was observed, the points are in pairs. The two gaps for each sample are represented by two symbols with the same shape at the same x, the solid symbol for Δ_π and the open symbol for Δ_σ. The points for this work at $x = 0$ are from Ref. [9].

er (see below). This suggests a comparison of a calculated λ with an "experimental" λ derived from Eq. (6) with the experimental γ and a calculated $N(E_F)$. Taking the calculated $N(E_F)$ as 0.710 states eV^{-1} $cell^{-1}$, and the experimental γ as 2.53 mJ K^{-2} mol^{-1}, the experimental λ is 0.52. The calculated values, which range from 0.61 to 0.88, are all higher. The De la Pena-Seaman et al. value, 0.672, is substantially higher. Their calculation was based on the assumption of harmonic phonons [33]. The phonons are actually anharmonic, and Choi et al. [14] found $\lambda = 0.61$ and 0.73 for anharmonic and harmonic phonons, respectively. (The calculation with the anharmonic phonons was also necessary to obtain agreement with the experimental T_c.) The calculated λ of Ummarino et al. was ~0.88. Other reported values include 0.88 [16]; 0.76 [13]; 0.72 [22]. The lowest of the calculated values, 0.61 [14], which seems to have been obtained with the most extensive consideration of the possibly relevant effects, corresponds to $\gamma = 2.69$ mJ K^{-2} mol^{-1}, just 6% greater than the experimental value. That difference is larger than the probable error in the experimental value, but making some allowance for uncertainty in the experimental value and taking the complexity of the calculation into account, the agreement of the experimental and theoretical values is certainly satisfactory.

For MgB_2 the calculated values of $N(E_F)$ for the individual bands cluster around $N_\pi(E_F)$ = 0.41 and $N_\sigma(E_F)$ = 0.30 states eV^{-1} $cell^{-1}$. Together with the values of γ_π and γ_σ, 1.16 and 1.37 mJ K^{-2} mol^{-1}, respectively, they suggest $\lambda_\pi = 0.20$ and $\lambda_\sigma = 0.94$ as the "experimental" values. The calculated values range from 0.395 to 0.630 for λ_π, and from 1.046 to 1.230 for λ_σ. They include, for λ_π and λ_σ, respectively, 0.395 and 1.046 [33]; 0.61 and 1.l2 [34]; 0.630 and 1.230 [17]; 0.45 and 1.19 [13]; 0.45 and 1.09 [22]. Whereas the calculated values of λ_σ are 10–30% higher than the experimental value, the calculated values of λ_π are higher by factors 2–3. This raises the question of possible experimental error in the relative values of γ_π and γ_σ. However, because λ_π and γ_σ add up to γ it is not possible to reduce the discrepancy for the π bands without increasing it for the σ bands by adjusting the values of γ_π and γ_σ. Furthermore the analysis of C_{es} into its two components gives values of Δ_π and Δ_σ that are in reasonable agreement with other results, which supports the validity of the values γ_π and γ_σ. A reasonable interpretation of the differences between the theoretical and experimental values of λ_π and λ_σ is that the calculations of the electron–phonon interaction on the π bands are less successful than for the relatively simple σ bands.

Band-structure calculations for carbon-doped MgB_2, unlike those for MgB_2 itself, give significantly different results for the values $N(E_F)$: For increasing x De la Pena-Seaman et al. [33] found small decreases in both $N_\pi(E_F)$ and $N_\sigma(E_F)$ that produce a decrease in $N(E_F)$ from 0.70 states eV^{-1} $cell^{-1}$ at $x = 0$ to 0.55 states eV^{-1} $cell^{-1}$ at $x = 0.1$. The calculations of Ummarino et al. [34] gave a reduction in $N(E_F)$ from 0.70 states eV^{-1} $cell^{-1}$ for $x = 0$ to 0.60 states eV^{-1} $cell^{-1}$ for $x = 0.1$, but in their calculation $N_\pi(E_F)$ decreases approximately linearly and $N_\sigma(E_F)$ is essentially constant for $x \leqslant 0.1$. Choi et al. [36] considered the case of $x = 0.1$, and found an even smaller decrease, in $N(E_F)$, only 10%. Consequently there are no well established values of $N(E_F)$ that could be used to define the "experimental" λ for comparison with calculated values. Instead, the experimental values of γ are compared with values derived from the calculated values of $N(E_F)$ and λ in Fig. 4. As shown there, the experimental γ_π is not strongly affected by carbon doping but the experimental γ_σ decreases steadily with increasing x. These trends are qualitatively consistent with the expected band filling effects on $N_\pi(E_F)$ and $N_\sigma(E_F)$ but they combine to give a conspicuous minimum in the experimental γ in the vicinity of $x = 0.05$ that is inconsistent with both of the theoretical results. The relatively good agreement between the two theoretical results, as they are represented in Fig. 4, however, is somewhat misleading: the underlying values of λ_π, λ_σ, $N_\pi(E_F)$, and $N_\sigma(E_F)$ and their dependences on x are significantly different. Accounting for the discrepancy between the experimental and theoretical results for the x dependence of γ on the basis of experimental error would require an error of the order of 0.7 mJ K^{-2} mol^{-1} in one or more of the values of γ. For undoped MgB_2 the value of γ is relatively well established, and Fig. 12 of Ref. [25] (specific heat measurements of another C-doped sample with $T_c \sim 20$ K) suggests that those results would give a value for γ similar to that reported here for $x = 0.1$. There is no obvious reason to expect an experimental error of the required magnitude for $x = 0.05$. Furthermore, as is made clear in Fig. 3, the correct values of the components of γ, γ_π and γ_σ, for both the $x = 0.05$ and 0.1 samples have to be close to those obtained in the two-gap analysis of C_{es}. Some experimental error is certainly possible, but the general lack of agreement among calculated values of λ, and, for carbon-doped samples, the lack of agreement among calculated values of $N(E_F)$ suggest that errors in the calculations may make a major contribution to the discrepancies between the experimental and theoretical values of γ.

The expected decrease in T_c with increasing x is apparent in Fig. 5. The values of T_c for the doped samples obtained from the specific heat measurements tend to be lower than those obtained by other measurements. This may be a consequence of the fact that the specific-heat T_c was taken as the midpoint of the transition in a bulk property, whereas other measurements are more likely to reflect the onset of superconductivity. The data of Gonnelli et al. [37] for T_c in Fig. 5 and for Δ_σ in Fig. 6a, which extend to $x = 0.13$, differ conspicuously from the Holanova/Szabo [38,39] and Tsuda et al. [40] data, which extend only to $x = 0.10$. In Fig. 6b, where Δ_σ is plotted vs T_c rather than x, the differences are reduced considerably. This shows that they are, at least in part, a consequence of a difference between the T_c and x relations in the Gonnelli data and those in the Holanova/Szabo and Tsuda data. In particular, they show that for a given T_c the value of x in the Gonnelli data is higher than in the Holanova/Szabo and Tsuda data. In this context, evidence that the upper limit of solubility of carbon in MgB_2 is $x = 0.10$ [41] is relevant. Kortus et al. [18] have argued that the decrease in T_c can be understood mainly as a band-filling effect. Starting with the band structure of undoped MgB_2 and the rigid-band approximation, they found an approximately linear decrease in T_c to $x \sim 0.05$. With several refinements, but without taking interband scattering into account, the linear region was extended to $x \sim 0.15$. Their result gave $T_c \sim 30$ K for $x \sim 0.1$, in reasonable agreement with the Gonnelli data but substantially higher than the other data in Fig. 5. (In several papers it has been emphasized that the Gonnelli data were obtained on single crystals. However, it should be noted that there are also single-crystal results [42] for which T_c is *lower* than any of the data in Fig. 5.) For $x \leqslant 0.1$ the calculation of De la Pena-Seaman et al. [33], which does not take interband scattering into account, gives a nonlinear dependence on x and a lower T_c, ~ 25 K at $x = 0.1$, in better agreement with the other data. The calculation of Ummarino et al. [34], which does take interband scattering into account, gives a result more like that of Kortus et al. [18], approximately linear in x and with $T_c \sim 30$ K at $x = 0.1$. The spread in the experimental data and the differences in theoretical calculations that give similar results preclude any conclusion about the role of interband scattering in determining the x dependence of T_c.

As shown in Fig. 6, the Gonnelli data for Δ_π and Δ_σ differ conspicuously from those of Holanova/Szabo and Tsuda. Regardless of the possibility raised above that the differences in the Δ_σ results reflect differences in the underlying T_c–x relations, the Gonnelli data are unique in giving evidence of a merging of the two gaps near $x = 0.132$, and $T_c = 18.9$ K. For that sample they saw only one gap. The specific-heat values for Δ_π and Δ_σ are in better agreement with the Holanova/Szabo and Tsuda data than the Gonnelli data. Together with the Holanova/Szabo and Tsuda data, they suggest that Δ_π decreases from $\sim$2.2 meV at $T_c = 39$ K to $\sim$1.4 meV at $T_c = 20$ K. In contrast, the Gonnelli Δ_π, together with the single gap they observe at $x = 0.132$, is approximately constant at $\sim$3 meV, which is essential to their conclusion that the gaps do merge. The preponderance of the experimental data suggests that if the gaps do become equal, it is at a value of x substantially higher than 0.1 that has not been reached (and which may be beyond the solubility limit of carbon). On the theoretical side, Kortus et al. [18] have interpreted the approximately constant Gonnelli Δ_π data as the net effect of the increase of Δ_π with increasing x that is expected for interband scattering (which was not included in their calculation of T_c) and the decrease expected for band filling. Qualitatively, the same interpretation could be made for the other Δ_π data in Fig. 6, which decrease slightly with increasing x. The calculation of De la Pena-Seaman et al. [33] is in better agreement with the Holanova/Szabo, Tsuda, and specific-heat data for Δ_π but in better agreement with the Gonnelli data for Δ_σ. It has the gaps merging only at $x = 0.175$, where they are both zero. Depending on whether interband scattering is included or not, and also on assumptions made about the x dependence of the Coulomb dependence, the Ummarino et al. calculation [34] gives a variety of re-

sults, including both approximate agreement with the Gonnelli data for both gaps and their merging near $x = 0.13$, and a result similar to that of De la Pena-Seaman et al. [33]. For the energy gaps, as well as for T_c, there are theoretical calculations that are in qualitative agreement with all of the experimental results. However, the similarity of the results of calculations based on different starting assumptions and the differences in the experimental results preclude any conclusions about the validity of those assumptions, and, therefore, about the degree to which they are supported by the experimental results.

5.2. Temperature-proportional term in the vortex state

The $\gamma_v(H)T$ term in the vortex-state heat capacity of MgB_2 is highly non-linear in H and, corresponding to the anisotropy of H_{c2}, anisotropic, i.e., dependent on θ, the angle of H with the c axis. Bouquet et al. [43] investigated these effects and gave a plausible interpretation: For $H \leqslant 0.5$ T, $\gamma_v(H, \theta)$ was isotropic, non-linear in H, and increased sharply with increasing H; for $H \geqslant 3$ T, it became anisotropic and linear in H. They interpreted these results on the basis of the difference in the coherence lengths, ξ_π and ξ_σ, for the π and σ bands: The spatial extent of the contribution of a band to the DOS at a vortex core is proportional to the coherence length, which, because of the small value of Δ_π, is much longer for the π band than the σ band. As a consequence, the π band makes a disproportionately large contribution to $\gamma_v(H)$ for each vortex, and the π-band DOS is "used up", i.e., its contribution to $\gamma_v(H)$ "saturates" at γ_π, at a relatively low H. Only the σ band contributes to the increase in $\gamma_v(H)$ for further increases in H. For low H, the π band makes the dominant contribution to $\gamma_v(H)$ and gives it the sharp initial increase; the lack of anisotropy is consistent with the 3D nature of the π-band Fermi surface. Bouquet et al. separated $\gamma_v(H, \theta)$ into contributions of the two bands, $\gamma_{v\pi}(H)$ and $\gamma_{v\sigma}(H, \theta)$, by attributing the linear-in-H behavior at high H to the σ band and extrapolating it to $H = 0$. They obtained $\gamma_{v\sigma}(H, \theta)$ as the extended straight line minus the intercept at $H = 0$, and $\gamma_{v\pi}(H)$ as the remainder of $\gamma_v(H, \theta)$, $\gamma_{v\pi}(H) = \gamma_v(H, \theta) - \gamma_{v\sigma}(H, \theta)$. The non-linearity was thus assigned entirely, but arbitrarily, to the π band. They reported the values of three critical fields, two for the σ band and one for the π band. Normally these would be defined as the H at which the corresponding contribution to $\gamma_v(H, \theta)$ saturates, but for the π band the nonlinearity of $\gamma_{v\pi}(H)$ precluded the use of that definition, and an extrapolation of the initial slope of $\gamma_{v\pi}(H)$ to γ_π was used to estimate $H_{c2\pi}$. (Later more precise and more extensive measurements by Pribulova et al. [44] gave similar results. Although they were described in a more complicated way, the analysis and interpretation were essentially the same as those of Bouquet et al. [43].

Fig. 7 shows the experimental $\gamma_v(H)$ data normalized to the normal-state EDOS by dividing by γ. With allowance for the fact that the measurements were made on polycrystalline samples, the results are qualitatively similar to those of Bouquet et al. [43] on MgB_2. Although their analysis was somewhat arbitrary, there is no theoretical basis for an alternative approach, and the same assumptions were used to separate the contributions of the two bands. On that basis the sharp increase in $\gamma_v(H)$ at low H was attributed to the small-gap π band, and the slower increase at higher H to the large-gap σ band. The separation of the contributions of the two bands involves the determination of four parameters. Two of these are the maximum contribution of each band to $\gamma_v(H)$. They were taken to be the same as the contributions to γ determined in the two-gap fit to C_{es}: $\gamma_\pi = 0.66\gamma$ and $\gamma_\sigma = 0.34\gamma$ for the $x = 0.05$ sample; $\gamma_\pi = 0.80\gamma$ and $\gamma_\sigma = 0.20\gamma$ for the $x = 0.1$ sample. The other two, which characterize the anisotropic H_{c2} of the σ band, are $H_{c2||ab}$ and the anisotropy parameter $\Gamma \equiv H_{c2||ab}/H_{c2||c}$. Together with γ_σ, they define $\gamma_{v\sigma}(H)$. Since the data are for a polycrystalline

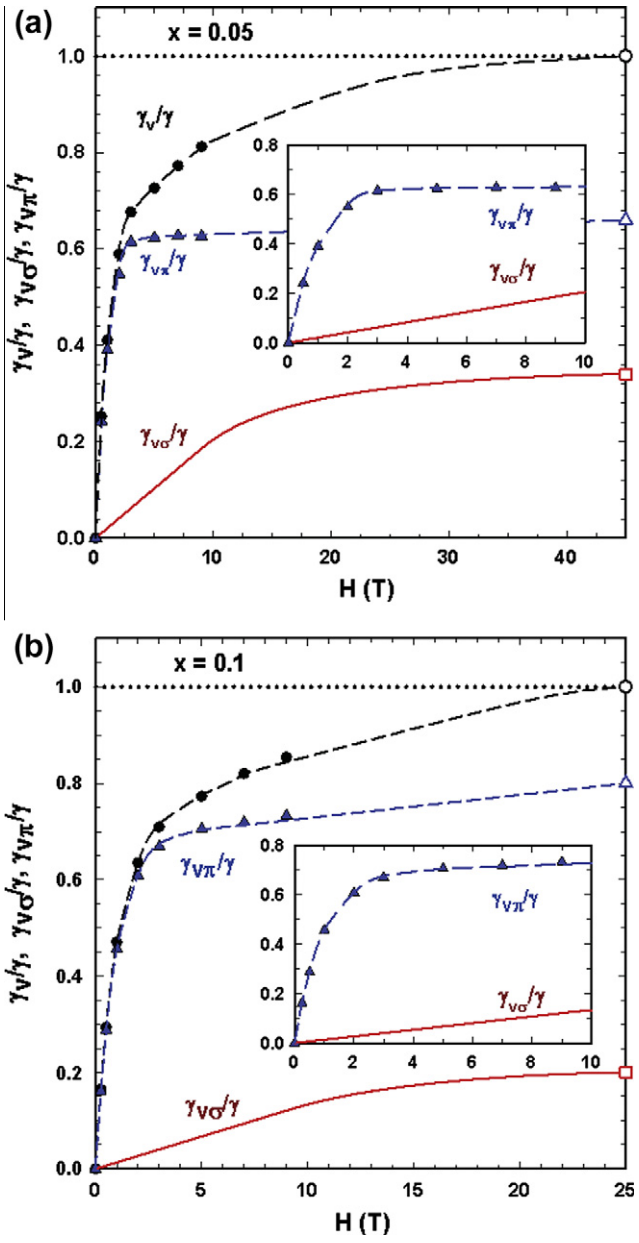

Fig. 7. The coefficient of the vortex-state, T-proportional term and the contributions of the σ and π bands, normalized to the normal-state value γ: (a) for $x = 0.05$; (b) for $x = 0.1$. The solid curved line, for $\gamma_{v\sigma}/\gamma$, was obtained by fitting the experimental data for $\gamma_v(H)$ for $H \geqslant 3$ T. The solid circles are the experimental data for $\gamma_v(H)/\gamma$, and the solid triangles are the corresponding points for $\gamma_{v\pi}(H)/\gamma$ obtained by subtracting $\gamma_{v\sigma}(H)/\gamma$. The open symbols on the right hand vertical axis are the normal-state values obtained in the two-gap fit to the superconducting-state data. The dashed curved lines are guides to the eye. See text for discussion.

sample with an assumed random orientation of the crystallites, $\gamma_{v\sigma}(H)$ is not linear in H, and the effective-mass model [45] was used to obtain the appropriate average of $H_{c2}(\theta)$ in terms of Γ and $H_{c2||ab}$. The values of those parameters were chosen to give the best approximation to the observed H dependence of $\gamma_v(H)$ for $H \geqslant 3$ T, where it is assumed to be that of $\gamma_{v\sigma}(H)$. The results are $H_{c2||ab} = 45$ T and $\Gamma = 5.0$ for the $x = 0.05$ sample, and $H_{c2||ab} = 25$ T and $\Gamma = 2.7$ for the $x = 0.1$ sample. The values of $H_{c2||ab}$ are somewhat higher than those reported elsewhere [30,31] but in view of the uncertainties in the various measurements the discrepancies are not surprising. The $\gamma_{v\sigma}(H)$ curves derived by fitting the experimental data for $\gamma_v(H)$ and $\gamma_{v\pi}(H)$, obtained as $\gamma_v(H) - \gamma_{v\sigma}(H)$ are also shown in Fig. 7.

6. Summary and conclusions

Specific-heat measurements on two samples of $Mg(B_{1-x}C_x)_2$, $x = 0.05$ and 0.1, characterize the evolution of the two-gap superconductivity with doping. The measurements give parameters characteristic of the individual π and σ bands, which are compared with other experimental results and with theoretical predictions of the effects of the band filling and increased interband scattering associated with the doping.

A two-gap analysis of the electron specific heat in the superconducting state determines the basic parameters characteristic of the individual bands, the energy gaps, Δ_π and Δ_σ, and the contributions to γ, γ_π and γ_σ. In combination with calculated values of the bare electron densities of states for the two bands, $N_\pi(E_F)$ and $N_\sigma(E_F)$, γ_π and γ_σ give "experimental" values of the electron–phonon coupling constants for the individual bands, λ_π and λ_σ. For the *undoped* MgB_2, the consistency of different calculated values of the *total* EDOS, $N(E_F) = N_\pi(E_F) + N_\sigma(E_F)$, gives confidence in that number. The resulting value of the total electron–phonon coupling constant, $\lambda = \lambda_\pi + \lambda_\sigma$, is in satisfactory agreement with one particularly rigorous calculation, but all other calculated values are substantially higher, as are the calculated values of λ_π and λ_σ, particularly λ_π. With increasing x, the experimental γ_π shows a weak minimum, the experimental γ_σ decreases substantially, and γ shows a distinct minimum. The two theoretical calculations are based on different approximations and give different values for the underlying values of the EDOS and electron–phonon interaction. Nevertheless, they give surprisingly similar results for γ_π, γ_σ, and γ. However, they differ substantially from the experimental results, most conspicuously in not showing the minimum in γ.

There is considerable scatter in the values of the critical temperatures for superconductivity and the energy gaps derived from other measurements, which is probably due at least in part to differences in the assigned values of x. The values derived from the specific-heat measurements fall within the limits defined by that scatter. All of the measurements show the substantial decrease in Δ_σ with increasing x that is expected as a consequence of both band filling and increased interband scattering, but the energy gaps obtained from other measurements fall into two distinct categories with respect to the merging of the gaps expected for interband scattering: one set of measurements shows the merging; two others give a different x dependence of Δ_π and no evidence of the merging. The specific-heat derived values of Δ_π are in good agreement with the latter, and suggest that the predicted merging does not occur, at least not within the range of x that has been investigated.

The temperature-proportional term in the vortex-state specific heat, which represents the contribution of the vortex cores, is highly nonlinear in H, reflecting both the different coherence lengths in the two bands and the anisotropy of the critical fields. An analysis analogous to that applied to single-crystal MgB_2, but allowing for the polycrystalline nature of the samples, gave values of the anisotropy and critical fields in reasonable agreement with those obtained in other measurements.

Acknowledgements

The work at Berkeley was supported by the Director, Office of Science, Office of Basic Energy Sciences, Materials Sciences and Engineering Division, U.S. Department of Energy, under Contract No. DE-AC02-05CH11231. N.O. also acknowledges support by the Deutsche Akademische Austauch Dienst. The work at Amherst College received support from the Dean of the Faculty's Emeriti Fund.

References

[1] J. Nagamatsu, J. Nakagawa, N. Muranaka, T. Zenitani, J. Akimitsu, Nature 410 (2001) 63.
[2] H. Suhl, B.T. Matthias, L.R. Walker, Phys. Rev. Lett. 3 (1959) 552.
[3] V.A. Moskalenko, Fiz. Met. Metalloved. 8 (1959) 503.
[4] B.T. Geilikman, R.O. Zaitsev, V.Z. Kresin, Sov. Phys. Solid State 9 (1967) 642; V.Z. Kresin, J. Low Temp, Physics 11 (1973) 519; V.Z. Kresin, S.A. Wolf, Physica C 169 (1990) 476.
[5] Y. Wang, T. Plackowski, A. Junod, Physica C 355 (2001) 179.
[6] F. Bouquet, R.A. Fisher, N.E. Phillips, D.G. Hinks, J.D. Jorgensen, Phys. Rev. Lett. 87 (2001) 04001.
[7] H. Padamsee, J.E. Neighbor, C.A. Shiffman, J. Low Temp. Phys. 12 (1973) 387.
[8] F. Bouquet, Y. Wang, R.A. Fisher, D.G. Hinks, J.D. Jorgensen, A. Junod, N.E. Phillips, Europhys. Lett. 56 (2001) 856.
[9] R.A. Fisher, G. Li, J.C. Lashley, F. Bouquet, N.E. Phillips, D.G. Hinks, J.D. Jorgensen, G.W. Crabtree, Physica C 385 (2003) 180.
[10] R.A. Fisher, N. Oeschler, N.E. Phillips, W.E. Mickelson, A. Zettl, CP850, Low Temperature Physics: 24th International Conference On Low Temperature Physics; in: Y. Takano, S. P. Hershfield, S. O. Hill, P. J. Hirschfeld, A. M. Goldman, (Eds.), 2006 American Institute of Physics, pp. 601–602.
[11] J.M. An, W.E. Pickett, Phys. Rev. Lett. 86 (2001) 4366.
[12] J. Kortus, I.I. Mazin, K.D. Belashchenko, V.P. Antropov, L.L. Boyer, Phys. Rev. Lett. 86 (2001) 4656.
[13] A.Y. Liu, I.I. Mazin, J. Kortus, Phys. Rev. Lett. 87 (2001) 87005.
[14] H.J. Choi, D. Roundy, H. Sun, M.L. Cohen, S.G. Louie, Phys. Rev. B 66 (2002) 020513.
[15] H.J. Choi, D. Roundy, H. Sun, M.L. Cohen, S.G. Louie, Nature 418 (2002) 758.
[16] T. Yildirim, O. Gulseren, J.W. Lynn, C.M. Brown, T.J. Udovic, Q. Huang, N. Rogado, K.A. Regan, M.A. Hayward, J.S. Slusky, T. He, M.K. Haas, P. Khalifah, K. Inumaru, R.J. Cava, Phys. Rev. Lett. 87 (2001) 037001.
[17] A.A. Golubov, J. Kortus, O.V. Dolgov, O. Jepsen, Y. Kong, O.K. Andersen, B.J. Gibson, K. Ahn, R.K. Kremer, J. Phys. Condens. Mat. 14 (2002) 1353.
[18] J. Kortus, O.V. Dolgov, R.K. Kremer, A.A. Golubov, Phys. Rev. Lett. 94 (2005) 027002.
[19] A.A. Golubov, I.I. Mazin, Phys. Rev. B 55 (1997) 15146.
[20] N. Schopohl, K. Scharnberg, Solid State Commun. 22 (1977) 371.
[21] A. Brinkman, A.A. Golubov, H. Rogalla, Phys. Rev. B. 65 (2002) 180517(R).
[22] I.I. Mazin, O.K. Andersen, O. Jepsen, O.V. Dolgov, J. Kortus, A.A. Golubov, A.B. Kuz'menko, D. van der Marel, Phys. Rev. Lett. 89 (2002) 107002.
[23] W. Mickelson, J. Cummings, W.Q. Han, A. Zettl, Phys. Rev. B 65 (2002) 052505.
[24] X. Huang, W. Mickelson, B.C. Regan, A. Zettl, Solid State Commun. 136 (2005) 278.
[25] R.A. Ribeiro, S.L. Bud'ko, C. Petrovic, P.C. Canfield, Physica C 384 (2003) 227.
[26] H. Schmidt, K.E. Gray, D.G. Hinks, J.F. Zasadzinski, M. Avdeev, J.D. Jorgensen, J.C. Burley, Phys. Rev. B. 68 (2003) 060508(R).
[27] C. Caroli, P.G. De Gennes, J. Matricon, Phys. Lett. 9 (1964) 307.
[28] R.R. Hake, Rev. Mod. Phys. 36 (1964) 124.
[29] O.V. Dolgov, R.K. Kremer, Phys. Rev. B 72 (2005) 024504.
[30] R.H.T. Wilke, P. Samuely, P. Szabo, Z. Holanova, S.L. Bud'ko, P.C. Canfield, D.K. Finnemore, Physica C 456 (2007) 108.
[31] M. Angst, S.L. Bud'ko, R.H.T. Wilke, P.C. Canfield, Phys. Rev. B 71 (2005) 144512.
[32] O. De la Pena-Seaman, R. de Coss, R. Heid, K.-P. Bohnen, Phys. Rev. B 79 (2009) 134523.
[33] O. De la Pena-Seaman, R. de Coss, R. Heid, K.-P. Bohnen, Phys. Rev. B 82 (2010) 224508.
[34] G.A. Ummarino, D. Daghero, R.S. Gonnelli, A.H. Moudden, Phys. Rev. B 71 (2005) 134511.
[35] A.H. Moudden, J. Phys. Chem. Solids 67 (2006) 115.
[36] H.J. Choi, S.G. Louie, M.L. Cohen, Phys. Rev. B 79 (2009) 094518.
[37] R.S. Gonelli, D. Daghero, A. Calzolari, G.A. Ummarino, V. Dellarocca, V.A. Stepanov, S.M. Kazakov, N. Zhigadlo, J. Karpinski, Phys. Rev. B 71 (2005) 060503(R).
[38] Z. Holanova, P. Szabo, P. Samuely, R.H.T. Wilke, S.L. Bud'ko, P.C. Canfield, Phys. Rev. B 70 (2004) 064520.
[39] P. Szabo, P. Samuely, Z. Pribulova, M. Angst, S. Bud'ko, P.C. Canfield, J. Marcus, Phys. Rev. B 75 (2007) 144507.
[40] S. Tsuda, T. Yokoya, T. Kiss, T. Shimojima, S. Shin, T. Togashi, S. Watanabe, C. Zhang, C.T. Chen, S. Lee, H. Uchiyoma, S. Tajima, N. Nakai, K. Machida, Phys. Rev. B 72 (2007) 064527.
[41] M. Avdeev, J.D. Jorgensen, R.A. Ribeiro, S.L. Bud'ko, P.C. Canfield, Physica C 387 (2003) 301.
[42] S. Lee, T. Masui, A. Yamamoto, H. Uchiyama, W. Tajimna, Physica C 397 (2003) 7.
[43] F. Bouquet, Y. Wang, I. Sheikin, T. Plackowski, A. Junod, Phys. Rev. Lett. 89 (2002) 257001.
[44] Z. Pribulova, T. Klein, J. Marcus, C. Marcenat, F. Levy, M.S. Park, H.G. Lee, B.W. Kang, S.I. Lee, S. Tajima, S. Lee, Phys. Rev. Lett. 98 (2007) 137001.
[45] R.C. Morris, R.V. Coleman, R. Bhandari, Phys. Rev. B 5 (1972) 895.